DINAME 2023 - Proceedings of the XIX International Symposium on Dynamic Problems of Mechanics,
A.S. De Paula, A.T. Fabro and M.R. Machado (Editors), ABCM.
Pirenópolis, Go, Brazil, February 26th to March 3rd, 2023

A Modular Prototype of a Pendular Accelerometer

Vinícius M. Maran[1], **Daniel S. Batista** [1], **Marcelo C. Tosin**[1] **and Francisco Granziera Júnior**[1]

[1] State University of Londrina, Electrical Engineering Department, Campus Universitário, Rod. Celso Garcia Cid, PR 445 km 380, CEP 86.057-970, Londrina, PR, Brazil.

Abstract: Pendulum accelerometers are highly complex sensors that combine a distinctive structural design and an exceedingly precise electronic system. This work proposes a modular prototype to assist the reproduction of a classic pendulum accelerometer, which allows the studying and development of these sensors. The platform was designed to enable integration tests, mechanical and electronic examination, and individual validation of each sensor's parts. The prototype built allows easy replacement of the mechanical elements, as well as entirely modular testing of the electronics. Results of the platform show that the mechanical studies are effective using the method, and separately addressing each electronic part allows for more straightforward solutions to the problem. Although the proposed prototype design has some limitations, it successfully served its purpose on multiple fronts and allowed a modular study of the pendulum accelerometer concept. Hence, it will allow for future studies on more advanced solutions for the mechanical parts of the sensor and the electronic system instrumentation.

Keywords: Pendular Accelerometer, Q-Flex, Acceleration measurement.

INTRODUCTION

The Q-Flex pendular force-feedback accelerometer sensors are well known and have an important role in the military, commercial, and scientific applications. Due to its wide measurement range, reliability, and performance, these sensors are applied in Inertial navigation systems (INS) used in different applications, such as satellite launchers, missiles, commercial and military airplanes, gun stabilization systems, directional drilling tools, among others. This type of sensor is also employed where the measurement of the specific reaction forces are directly proportional to other quantities, such as in the Cassini-Huygens mission where the Huygens probe measured the Titan's atmospheric density profile during its descend (Hathi *et al.*, 2009). Another scientific application is its use to characterize small specific forces found in a microgravity ambient such as at the microgravity facilities in the International Space Station and in a rocket launched microgravity platform (Tosin *et al.*, 2010), for example.

Several Q-Flex sensor models are available on the market, with different sizes, acceleration ranges, and performance capabilities. They have a precisely balanced design with performance characteristics far superior in bias and scale factors compared to other accelerometer topologies. Usually, those are high-end sensors at a high cost. All are torque-to-balance servo electromagnetic accelerometers featuring a quartz pallet. Those are very complex sensors with specific construction aspects, and their reproduction is not straightforward. Thus, considering their applications and the different characteristics of the sensor, this work proposes a modular prototype of a pendular accelerometer. The prototype is used to assist in designing and constructing a high-accuracy and performance sensor. In addition, the proposed modularity allows focusing on the development of specific parts of the accelerometer at a lower cost instead of a fully integrated design.

The pendular architecture was widespread in the late 1960s with the first high-efficiency designs published by Wilcox (U.S. Patent 3,229,53, Nov. 1960), Jacobs (U.S. Patent 3,702,07, Feb. 1969), and Rogall (U.S. Patent 3,513, 711, Feb. 1969). Although the technology has been known for a relatively long time and current technology allows for reproducing optimized and high-reliability accelerometers, designing and building such a sensor is a technological and electronic challenge. Furthermore, different from the first models, it is now possible to implement and control the accelerometers digitally (Zwahlen *et al.*, 2016). The main goal of the work is to design and assemble a modular prototype based on the patent of Jacobs (U.S. Patent 3,702,07, Feb. 1969). This will allow for evaluating and modeling the sensor so that it can be integrated with compatible electronics. In turn, the final prototype will allow for assessing its accuracy and performance and designing new optimized accelerometers, especially in size.

Jacobs' Patent Accelerometer Concept

The prototype concept is based on Jacobs' patent 3,702,073, which has its accelerometer design illustrated in Fig. 1. The proof-mass annular plate supports the quartz pendulum structure. The plate is attached to the sensor's outer structure by a pair of hinges. The hinge structure acts as a coil, generating a force that opposes the proof mass movement. Each side composes a plate that forms a differential capacitive position sensor to measure the pendulum position and provide a feedback signal to the servo. The servo inserts a current through quartz pendulum-proof coils that interact with the magnetic field of the permanent magnets to provide the electromechanical torque, which closes the servo loop and maintains the proof mass fixed at its null position. The imposed acceleration is linearly proportional to the feedback current within these conditions.

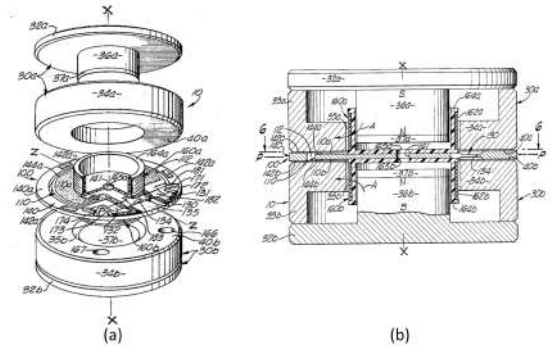

Figure 1 – (a) Exploded view showing parts of the accelerometer. (b) Cross-sectional view of the accelerometer unit.

MODULAR PROTOTYPE CONCEPT AND MECHANICAL DESIGN

The design of the modular prototype is depicted in Figure 2 and is in accordance with the Q-Flex topology outlined in the patent by Jacobs (U.S. Patent 3,702,07, Feb. 1969). The prototype comprises all the essential elements of the Q-Flex topology such as permanent magnets, capacitive plates, coils, and a proof-mass ring. However, it does not incorporate an external shield to return the magnetic field flux. This configuration enables the individual elements of the system to be studied independently. Additionally, the prototype structure employs a transparent acrylic material as a cost-effective solution that can withstand the magnetic repulsion force while not influencing the electromagnetic field.

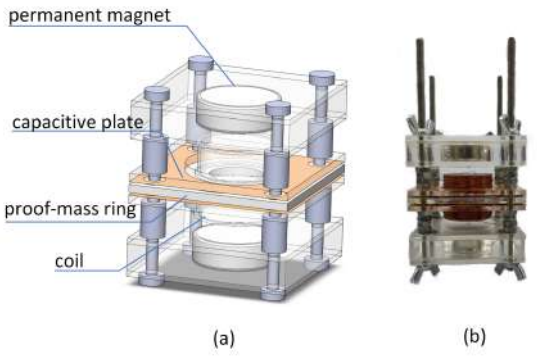

Figure 2 – (a). Modular Prototype Project design for validate the main concepts of a pendular accelerometer. (b). Modular Prototype built and assembled.

The Proof Mass Ring

The flapper is a crucial component of a Q-Flex accelerometer, responsible for converting mechanical motion into an electrical signal that can be measured. The design of the flapper involves several factors, including sensitivity, frequency range, and environmental conditions. For example, a highly sensitive flapper can detect small accelerations but may not be as durable as one made of a more robust material. The flapper is usually a one-piece hinge and pendulum structure, often made of a stable material such as fused quartz. This material is non-conductive and has a low coefficient of thermal expansion, which helps to minimize the change in a pendulum motion with temperature Lawrence (2001).

Flexure-hinged designs, such as notch flexures, are common in precision engineering applications due to their advantages, including smooth and repeatable motion, low friction losses, and not requiring maintenance. However, as discussed in Henning *et al.* (2018), the motion behavior and deformation can be complex to develop an accurate elastic-kinematic.

Figure 3 illustrates the parameters of a symmetric corner-filleted Flexure Hinge, according to Lobontiu (2002). The hinge's thickness, $t(x)$, is determined in terms of the fillet radius r and the flexure length l, given by Eq.1.

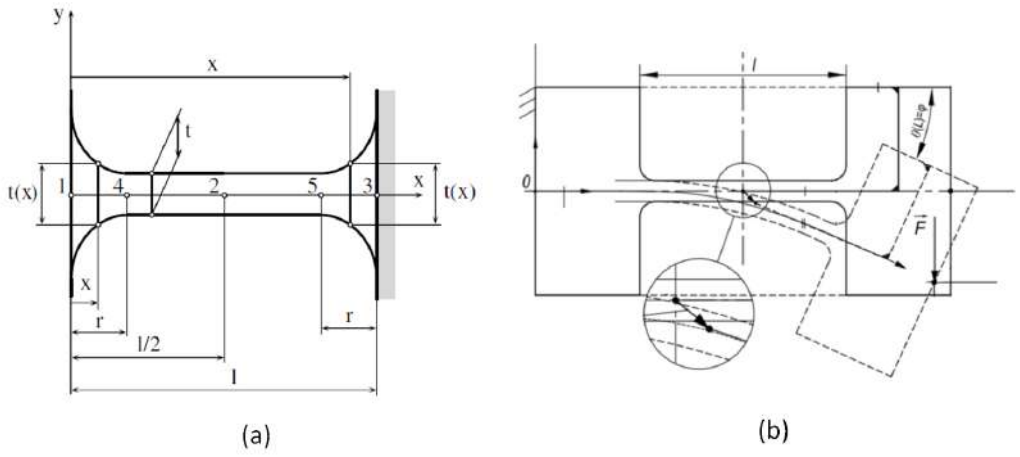

Figure 3 – (a). Cross-sectional profile of a symmetric corner-filleted flexure hinge; (b). Cross-sectional of a flexure hinge deflection.

$$t(x) = \begin{cases} t + 2\cdot\left[r - \sqrt{x\cdot(2\cdot r - x)}\right], & x \in [0, r] \\ t, & x \in [r, l-r] \\ t + 2\cdot\left[r - \sqrt{(l-x)\cdot[2\cdot r - (l-x)]}\right], & x \in [l-r, r] \end{cases} \tag{1}$$

The hinge is an essential part of the flapper's design and requires an analytical approach to model and evaluate the impact of its different parameters on performance. The rotation capacity considered was considered in the development of the design of the test mass ring, whose rotation capacity in the x and y axis can be expressed by the equations 2 and 3.

$$C_{1,x-F_x} = \frac{1}{Ew}\cdot\left[\frac{l-2r}{t} + \frac{2(2r+t)}{\sqrt{t(4r+t)}}\cdot\arctan\left(\sqrt{1+\frac{4r}{t}} - \frac{\pi}{2}\right)\right] \tag{2}$$

$$\begin{aligned} C_{1,y-F_y} = \frac{3}{Ew}\Bigg\{ & \frac{4(l-2r)\left(l^2 - lr + r^2\right)}{3t^3} + \frac{\sqrt{t(4r+t)}\left[-80r^4 + 24r^3t + 8(3+2\pi)r^2t^2 + 4(1+2\pi)rt^3 + \pi_t^4\right]}{4\sqrt{t^5(4r+t)^5}} + \\ & \frac{(2r+t)^3\left(6r^2 - 4rt - t^2\right)}{\sqrt{t^5(4r+t)^5}}\arctan\sqrt{1+\frac{4r}{t}} + \frac{-40r^4 + 8lr^2(2r-t) + 12r^3t + 4(3+2\pi)r^2t^2 + 2(1+2\pi)rt^3 + \frac{\pi t^4}{2}}{2t^2(4r+t)^2} \\ & + \frac{4l^2r\left(6r^2 + 4rt + t^2\right)}{t^2(2r+t)(4r+t)^2} - \frac{(2r+t)\left[-24(l-r)^2r^2 - 8r^3t + 14r^2t^2 + 8rt^3 + t^4\right]}{\sqrt{t^5(4r+t)^5}}\arctan\sqrt{1+\frac{4r}{t}}\Bigg\} \end{aligned} \tag{3}$$

Based on that, acrylic can be a suitable material for the flapper in a low-cost prototype, as it is relatively inexpensive and easy to tailor. However, it has some limitations, such as a relatively low natural frequency and a high coefficient of thermal expansion, unlike quartz. These limitations were considered when developing the prototype and may impact the accelerometer's overall performance compared to other materials design. A workaround to reduce these limitations was to design the hinge of the flapper with a low spring rate, which allows the flapper to move freely in response to acceleration. This can improve the overall sensitivity of the accelerometer. Therefore, employing an acrylic-based solution is justified as a cost-effective solution for this stage of development and allows testing and improvements at a reduced cost and development time. Other materials shall be considered for future versions of the product.

The Magnetic Field

As stated in Jacobs (U.S. Patent 3,702,07, Feb. 1969), the Q-Flex accelerometer uses pairs of permanent magnets to generate a magnetic field that is used to detect motion. Typically, the magnets are made of a material such as neodymium or samarium-cobalt, which have a very high magnetic field strength. The magnets are arranged in pairs symmetrically at each end of the accelerometer. The magnets selected for the bench test are of NdFeB composition, N35 grade capable of

supplying 0.34 T. Neodymium magnets can be brittle and can be easily damaged if they collide with each other, so two pieces were designed to contain the counterflow neodymium magnets.

The strength of the magnetic field generated by the magnets is a crucial factor in determining the accelerometer's sensitivity and resolution. By using high-strength magnets, the sensor can detect even small accelerations. However, it's important to note that the magnets used in the Q-Flex accelerometer may be affected by external magnetic fields, which can cause errors in the accelerometer's output. Therefore, pole pieces are designed to shield the external magnetic fields and provide a return path for the internal magnetic field.

Pole pieces are usually made of a high-permeability magnetic material such as permalloy or mu-metal. These materials have very high magnetic permeability, so they can effectively channel the internal magnetic field while blocking external magnetic fields. In addition, the pole pieces are typically arranged around the magnets to form a closed magnetic circuit. Such an arrangement ensures that the internal magnetic field is confined within the accelerometer and does not leak into the surrounding environment. It also helps reduce external magnetic fields' effects on the accelerometer's output.

High permeability magnetic materials like mu-metal or permalloy tend to be more expensive than others; hence, we opted for a modular prototype design without the pole pieces. The prototype's purpose is to allow several tests and observe the sensor's dynamics, and it is vital to consider the trade-offs between cost and performance. Therefore, to reduce the impact of the external magnetic field on the accelerometer's output, the prototype should be placed the accelerometer in an environment with minimal magnetic fields or use shielding techniques during the tests. The latter is done by enclosing the system in a non-magnetic metallic enclosure.

Simulating the magnetic flux of counterflow permanent magnets can be helpful in understanding and optimizing the performance of a Q-Flex accelerometer. The magnetic field generated by this element is illustrated in Fig. 4. It is possible to note the high-density magnetic field in the area between the magnets where the north and south poles are facing each other. By simulating the magnetic flux, it is possible to analyze how the magnetic field strength affects the sensitivity and resolution of the accelerometer and make adjustments to optimize its performance.

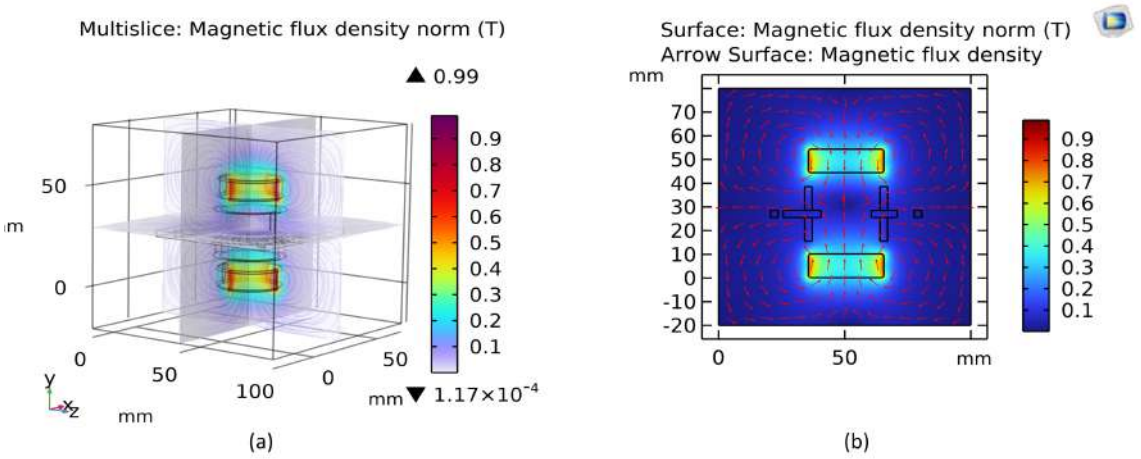

Figure 4 – Simulation to study the behavior of magnetic flux density norm provided by the pair of permanent magnetics: (a) multislice view (b) planar view.

The Movement Sensing Capacitors

The capacitance of the capacitors is a crucial parameter in determining the sensitivity and resolution of the Q-Flex accelerometer. In the prototype, the proof-mass ring was coated with copper on opposite surfaces to create differential capacitor plates. Copper is a suitable conductor of electricity and is commonly used as a material for the plates of capacitors.

As a result, a capacitor was formed on each side of the ring. When the accelerometer experiences acceleration, the test mass ring moves, causing a change in the capacitance of one plate and an opposite change in the capacitance of the other plate. To maximize the system's capacitance changes sensitivity, the three components were positioned closely together, allowing for the detecting of small variations in capacitance.

Simulations were conducted to study the behavior of the capacitance as a function of the displacement of the test mass and to predict the sensitivity and resolution of the accelerometer. The simulation results were illustrated in Figure 5 (a). However, the experimental results indicated that the capacitance values observed in the 14-17 pF range were significantly lower than the simulation results. This discrepancy may be attributed to mechanical issues such as misalignment of the copper-coated surfaces, which can severely impact the accelerometer's accuracy.

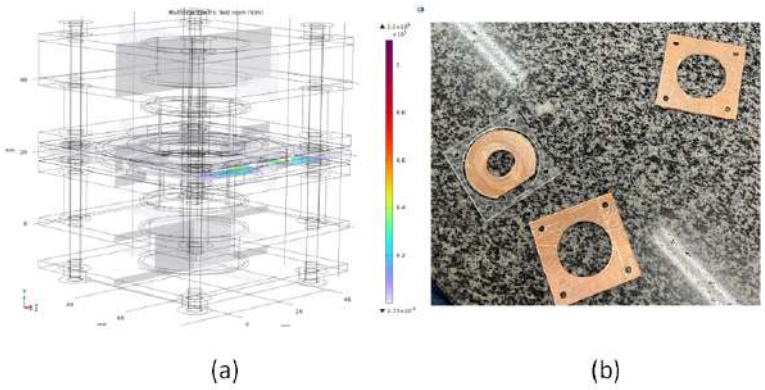

Figure 5 – (a). Multislice View of the Prototype capacitance simulation; (b) Copper-coated built parts of the modular prototype.

The Actuators – A Pair of Coils

A pair of coils are placed on each side of the plate to act as the accelerometer's actuator. It seeks to maintain stability and counteract the tendency for the capacitance to fluctuate. The coils can be used to return the flapper to its original position by applying a current through the coils' wire that creates a magnetic field counteracting the magnetic field of the permanent magnets. This allows for a closed-loop system where the flapper's position can be controlled and maintained. Fig 6 shows the simulation of the magnetic field flux during current flow.

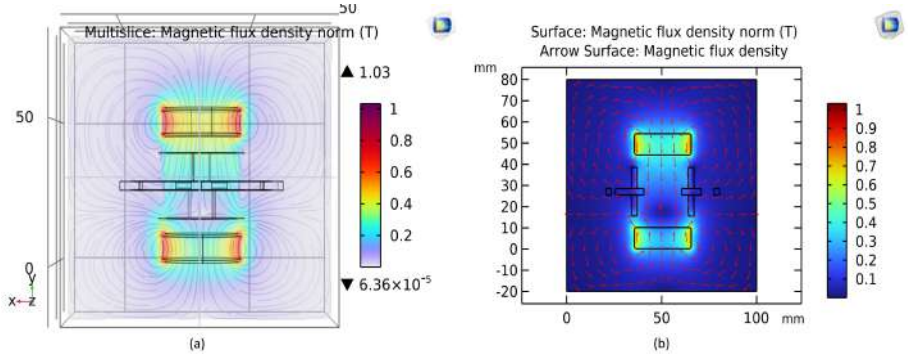

Figure 6 – Simulation of Magnetic field flux to study coil the coil interaction with the permanent magnetics. (a) Multislice view (b) planar view.

The torque provided by the coils can be calculated by the product of the magnetic flux density, B, the current through the wires, i, the number of turns, N, and the coil diameter, d, as shown in Eq. 4.

$$\tau = \pi \cdot B \cdot i \cdot N \cdot d \tag{4}$$

A potential issue with the design of the actuator is the difficulty in dissipating the heat generated by the electrical current flow in the coils. This problem is particularly challenging in the pendulum accelerometer due to a high thermal impedance. Although the hinge can conduct heat, it has a higher resistance path, and consequently, the conduction through the coils' copper wire is the primary heat dissipation method. However, the copper wire has a relatively high expansion coefficient, which can cause damage to the prototype if temperatures become too high. The design must address that considering the resistance of the wire, shown in Eq. 5:

$$R = \rho \cdot N \cdot \pi \cdot d \cdot (\frac{1}{4}\pi d_w), \tag{5}$$

where the resistance is proportional to the length of the wire and inversely proportional to the cross-sectional wire area, ρ is the wire material resistivity, and d_w is the wire diameter.

One way to achieve an optimum actuator design is to minimize the heat generated while maximizing the force generated; hence, it must take into account the wire resistivity changes with temperatures to reduce the wire resistance increase

with temperature. The actuator design should dissipate heat effectively while using a wire with a low coefficient of thermal expansion. These can reduce the potential damage to the coils and thermal runaway. It is also important to choose a wire with a low resistivity to minimize power dissipation and use a wire with a large cross-sectional area to maximize force generation. By carefully pondering these factors, it is possible to design an actuator that generates a high force per watt dissipated.

Another constraint in the design is that the air gap affects the magnetic flux density, B, in the coils of an accelerometer. The allowable size of the accelerometer and the magnetic material's properties limit the coil's size. The actuator must balance the flux density, the coils' size, and the resistance to generate the highest force per unit of power to achieve the best performance. This matter is addressed in more detail in the reference Lawrence (2001). For that, the actuator must combine equations 4, 5, and empirical magnet simulations to project the optimal coil inductance.

In the Q-Flex accelerometer topology, the current passes across the hinge through a thin metal conducting layer. Therefore, it is imperative to ensure that power is conducted through the coils of the Q-Flex topology without causing any torque on the pendulum. This constraint exists because if the metal layer conducting the current through the hinge is not the same thickness on both sides, the different expansion coefficients will create torque and cause the instrument bias to change with temperature.

The Pendular Accelerometer Dynamic Model

A dynamic model is a mathematical representation of a system that describes how the system behaves over time. It typically involves a set of differential equations that describe the relationships between different variables within the system and how they change over time.

The sensor can be modeled as a lateral pendulous mass, denoted by m, which is attached to an elastic hinge with a spring constant of k and is situated in a viscous environment with a constant coefficient of viscosity, represented by B. The displacement of the test mass, as indicated by the differential capacitors modeled by G_x, is maintained at the central position by applying a counterforce generated by a feedback current. Figure 7 shows a block diagram summarizing this dynamic model.

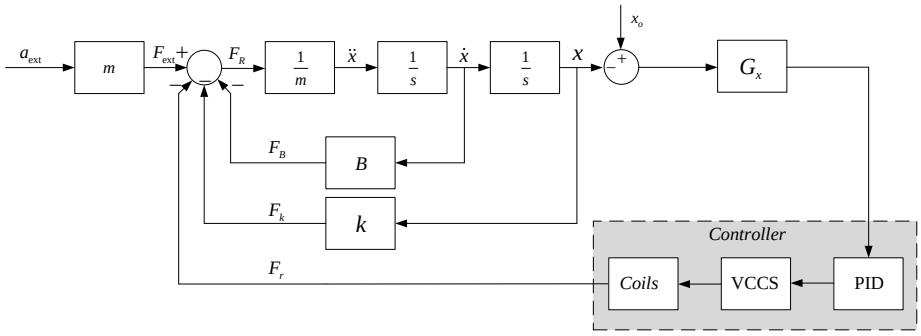

Figure 7 – Simplified dynamic model diagram of the proposed modular prototype of a pendular accelerometer.

The deflection of the test mass m, denoted here by $X(s)$ at Laplace domain, in response to the force to which it is subjected is given by Eq. 6. Where a_{ext} is the Newtonian acceleration applied to the sensor Merhav (1998).

$$\frac{X(s)}{A_{\text{ext}}(s)} = \frac{1}{s^2 + \left(\frac{B}{m}\right)s + \frac{K_{eq}}{m}} \tag{6}$$

where K_{eq} a constant that joins $K + G \cdot K_p$, the controller constant is K_p assuming it is only proportional.

MODULAR ELECTRONIC DESIGN CONCEPT

We approached the design of each circuit system independently to preserve the modular nature of the prototype. That concept allows for making subtle modifications or even replacing each system entirely. The following subsections discuss each electronic circuit.

Capacitance Measurement

Using a differential capacitor configuration can help improve the performance of the accelerometer by canceling out common mode noise, which is common to both plates. However, the capacitance value of the plates must be matched to

within a certain tolerance to achieve this noise cancellation.

The system responsible for measuring the acceleration inertia is described in the diagram in Fig. 8, where the variable capacitor C is arranged in a differential capacitance. Each plate capacitance is indicated by $C+\Delta C$ and $C-\Delta C$. This circuit is a high-frequency oscillator whose voltage is applied to the capacitive surfaces. The main idea is to accurately measure the displacement of the plates along the central axis by reading the amplitude of the output signal.

The capacitance (pF) of a single plate in a vacuum with surface A and a gap of x is given by the equation 7.

$$C = \frac{0.225 \cdot A}{x}, \tag{7}$$

and the rate of change of capacitance with distance is given by Eq. 8.

$$\frac{\partial C}{\partial x} = -\frac{0.225 \cdot A}{x^2} \tag{8}$$

For small capacitance variations, it can be assumed that

$$\Delta C = -C\frac{\Delta x}{x} \tag{9}$$

The superposition principle can be used to estimate the contribution of each source in the system and to establish the relationship between the input and output of the circuit. Isolating the 180 degrees out of phase source, Eq. 10 and calculating its contribution, we have Eq. 11.

$$V_{out}^{+} = \frac{V_{in} \cdot (C+\Delta C)}{4 \cdot C} \tag{10}$$

$$V_{out}^{-} = -\frac{V_{in} \cdot (C-\Delta C)}{4 \cdot C} \tag{11}$$

Combining both Eq. 10, Eq. 11, and Eq. 9 the output expression is obtained. This relation is seen in Eq. 12.

$$V_{out} = V_{out}^{+} + V_{out}^{-} = \frac{2 \cdot V_{in} \cdot \Delta C}{4 \cdot C} = \frac{V_{in}}{2} \cdot \frac{\Delta C}{C} = -\frac{V_{in}}{2} \cdot \frac{\Delta x}{x} \tag{12}$$

The sensor's sensitivity is inversely proportional to the gap between the plates, as demonstrated by equation 7. Additionally, the output capacitance, as outlined in equation 12, is also affected by an increase in the input voltage, V_{in}.

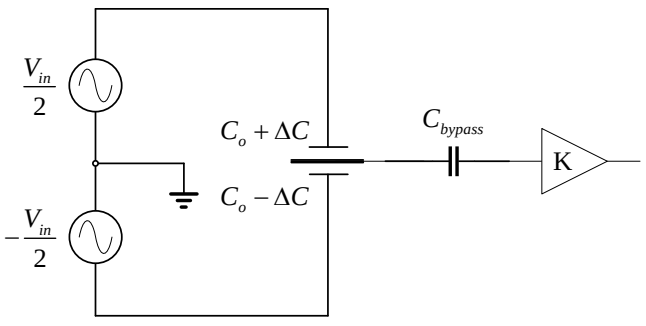

Figure 8 – Capacitance bridge for measurement of proof mass displacement.

In the prototype, the alternated signal is provided by a high-speed DAC. Fig. 9 shows the proposed circuit based on the previous diagram Fig. 8. Ideally, the distance between the top and bottom plates would be the same distance from the proof mass ring, resulting in a null output in this system. Consequently, for any changes in the x gap, the phase of V_o changes by 180 degrees. Also, the greater the imbalance between the plates, the higher the amplitude of the resulting signal. To cope with a signal that might have very low magnitudes, a bypass capacitor is added to filter out noise interference and improve reliability in the reading.

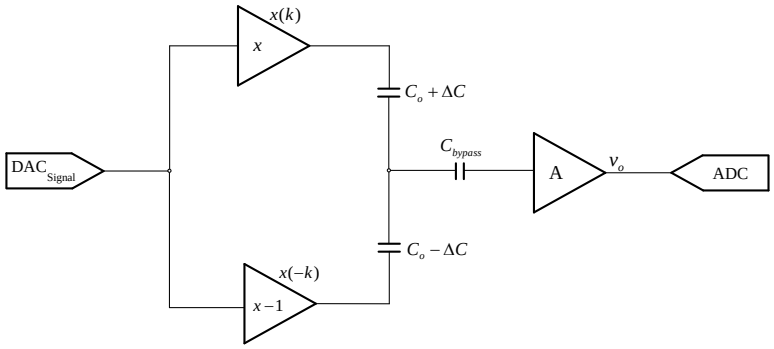

Figure 9 – Diagram of the Capacitance Modulated Peak-to-Peak Voltage Circuit.

Coils Actuators

The coils close the sensor loop by providing torque against acceleration. The test mass ring can be over-tensioned for both the top and bottom gaps in the pendulum accelerometer design. Therefore, the circuit that powers the coils must be able to deliver a symmetrical current through the actuator as linear and accurately as possible.

A voltage-controlled current source (VCCS) is suitable for controlling the actuator's current. This source topology allows a microcontroller (responsible for the digital control) to handle the VCCS current using a DAC. The Howland Current Source (HCS) was chosen among available topologies. The HCS is used in many applications and can provide a symmetric current regardless of the load's impedance value. In addition, its design is highly simplistic, uses only one Operational Amplifier, and allows a linear solution to the voltage-controlled current source problem, which has a few advantages over more complex topologies (Batista *et al.*, 2023).

Fig. 10 shows the schematic of the Howland Current Source circuit to supply the design actuator.

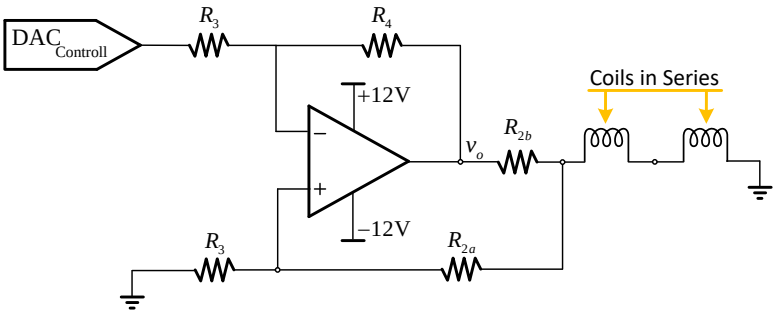

Figure 10 – Schematic of the Howland Current Source to supply current through the coils.

PROTOTYPE VALIDATION INITIAL RESULTS

The modular prototype has served well in the proposal of allowing tests and modifications quickly and simply. The next steps are to identify the model's constants and design an electronic controller for the sensor.

The application of current to the coil system allows for the study of the response of the capacitive system, as illustrated in Figure 11. The output data was collected using an oscilloscope, which allowed for real-time observation of the signal resulting from the variations and measurement of the peak-to-peak voltage. It was observed that the data described a parabolic shape, indicating that there was a phase shift present. This phenomenon occurred due to the curvature of the plates towards the lower axis of the sensor, caused by the influence of gravity. Furthermore, upon further examination, it was noted that when the current in the coils reached 0.8 A, the actuator overcame the barrier of gravity in the test mass, and the smallest voltage value at the output was observed when the ring was in the center position. Subsequently, as the current increased, the ring shifted to the upper axis, which was denoted by the phase shift and the increase in peak-to-peak voltage.

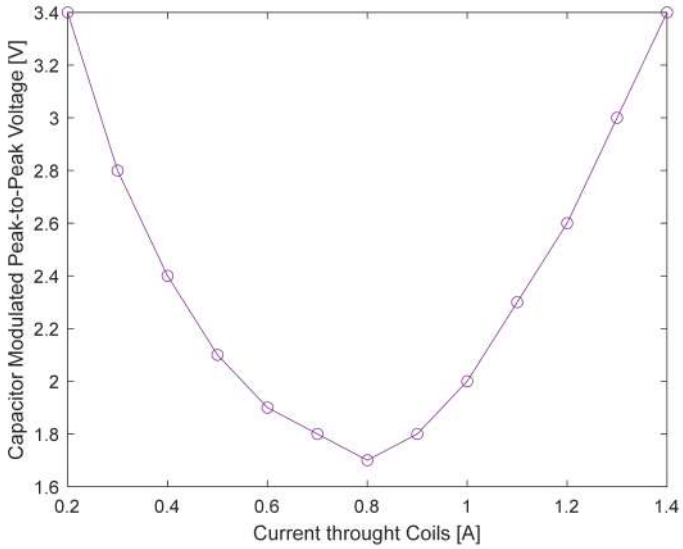

Figure 11 – Capacitance Modulated Peak-to-Peak Voltage Response.

CONCLUSION

The experimental validation of the proposed modular prototype was essential in the testing process and revealed its limitations. Furthermore, the current design's development and its limitations led to valuable insights for the future development of a more advanced version of the pendulum accelerometer closer to the intended concept. A new prototype can guarantee the desired performance and functionality level by addressing the current design's shortcomings.

The proposed current source demonstrated its capability by successfully moving the test mass ring within the prototype, as shown by the response curve of the differential capacitive circuit. It is worth noting that the system operates in a closed loop, and therefore, the current range should be kept within a more moderate range to avoid excessive power consumption. The wide range of responses of the system demonstrates its ability to operate over a large scale. However, it is desirable to operate within a linear region for greater precision and reliability. Future improvements should aim to reduce the gap between the plates to increase the sensitivity to inertial forces.

ACKNOWLEDGMENTS

This work was supported by the Coordenação de Aperfeiçoamento de Pessoal de Nível Superior - Brazil (CAPES) - Finance Code 001.

REFERENCES

Batista, D.S., Granziera, F., Tosin, M.C. and de Melo, L.F., 2023. "Analysis and practical implementation of a high-power howland current source". *Measurement*, Vol. 207, p. 112404. ISSN 0263-2241. doi: https://doi.org/10.1016/j.measurement.2022.112404.

Hathi, B., Ball, A., Colombatti, G., Ferri, F., Leese, M., Towner, M., Withers, P., Fulchigioni, M. and Zarnecki, J., 2009. "Huygens hasi servo accelerometer: A review and lessons learned". *Planetary and Space Science*, Vol. 57, No. 12, pp. 1321–1333.

Henning, S., Linß, S. and Zentner, L., 2018. "detasflex–a computational design tool for the analysis of various notch flexure hinges based on non-linear modeling". *Mechanical Sciences*, Vol. 9, No. 2, pp. 389–404.

Jacobs, E.D., U.S. Patent 3,702,07, Feb. 1969. "Accelerometer".

Lawrence, A., 2001. *Modern inertial technology: navigation, guidance, and control*. Springer Science & Business Media.

Lobontiu, N., 2002. *Compliant mechanisms: design of flexure hinges*. CRC press.

Merhav, S., 1998. *Aerospace sensor systems and applications*. Springer Science & Business Media.

Rogall, H., U.S. Patent 3,513, 711, Feb. 1969. "Accelerometer".

Tosin, M.C., Granziera Jr, F. and de Souza, L.G.G., 2010. "Design and operating limits of the platform for acquisition of acceleration data (paanda)". In *IAC 2010 congress proceedings, 61st International Astronautical Congress (IAC)*. Prague, Czech Republic.

Wilcox, D.E., U.S. Patent 3,229,53, Nov. 1960. "Accelerometer".

Zwahlen, P., Balmain, D., Habibi, S., Etter, P., Rudolf, F., Brisson, R., Ullah, P. and Ragot, V., 2016. "Open-loop and closed-loop high-end accelerometer platforms for high demanding applications". In *2016 IEEE/ION Position, Location and Navigation Symposium (PLANS)*. IEEE, pp. 932–937.

RESPONSIBILITY NOTICE

The author(s) is (are) the only responsible for the printed material included in this paper.